Sisyphus cooling and amplification by a superconducting qubit

M. Grajcar[1,2], S.H.W. van der Ploeg[1], A. Izmalkov[1], E. Il'ichev[1],
H.-G. Meyer[1], A. Fedorov[3], A. Shnirman[4], and Gerd Schön[5]
[1]*Institute of Photonic Technology, P.O. Box 100239, D-07702 Jena, Germany*
[2]*Department of Experimental Physics, Comenius University, SK-84248 Bratislava, Slovakia*
[3]*Quantum Transport Group, Delft University of Technology, 2628CJ Delft, The Netherlands*
[4]*Institut für Theoretische Physik, Universität Innsbruck, A-6020 Innsbruck, Austria*
[5]*Institut für Theoretische Festkörperphysik and DFG-Center for Functional Nanostructures (CFN), Universität Karlsruhe, D-76128 Karlsruhe, Germany*

Laser cooling of the atomic motion paved the way for remarkable achievements in the fields of quantum optics and atomic physics, including Bose-Einstein condensation and the trapping of atoms in optical lattices. More recently superconducting qubits were shown to act as artificial two-level atoms, displaying Rabi oscillations, Ramsey fringes, and further quantum effects[1,2,3]. Coupling such qubits to resonators[4,5,6,7] brought the superconducting circuits into the realm of quantum electrodynamics (circuit QED). It opened the perspective to use superconducting qubits as micro-coolers or to create a population inversion in the qubit to induce lasing behavior of the resonator[8,9,10,11]. Furthering these analogies between quantum optical and superconducting systems we demonstrate here Sisyphus cooling[12] of a low frequency LC oscillator coupled to a near-resonantly driven superconducting qubit. In the quantum optics setup the mechanical degrees of freedom of an atom are cooled by laser driving the atom's electronic degrees of freedom. Here the roles of the two degrees of freedom are played by the LC circuit and the qubit's levels, respectively. We also demonstrate the counterpart of the Sisyphus cooling, namely Sisyphus amplification.

For red-detuned high-frequency driving of the qubit the low-frequency LC circuit performs work in the forward and backward part of the oscillation cycle, always pushing the qubit up in energy, similar to Sisyphus who always had to roll a stone uphill. The oscillation cycle is completed with a relaxation process, when the work performed by the oscillator together with a quantum of energy of the high-frequency driving is released by the qubit to the environment via spontaneous emission. For blue-detuning the same mechanism creates excitations in the LC circuit with a tendency towards lasing and the characteristic line-width narrowing. In this regime "lucky Sisyphus" always rolls the stone downhill. Parallel to the experimental demonstration we analyze the system theoretically and find quantitative agreement, which supports the interpretation and allows us to estimate system parameters.

The system considered is shown in the inset of Fig. 1. It consists of a three-junction flux qubit[13], with the two qubit

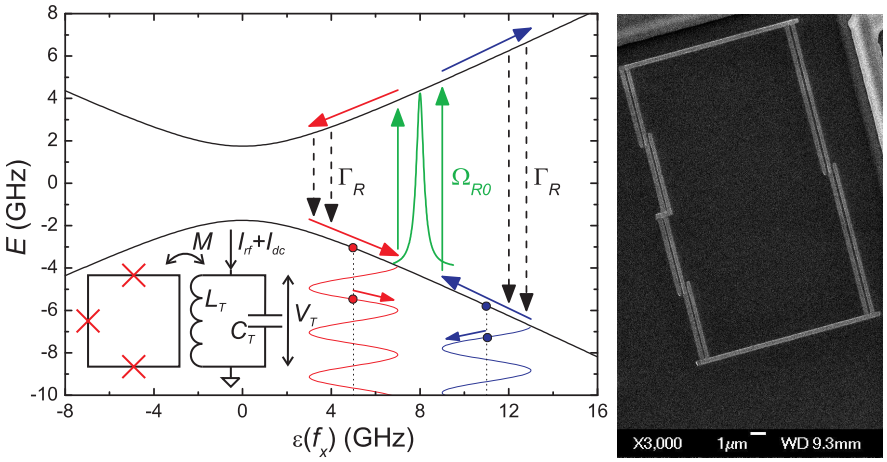

FIG. 1: **(a)** The energy levels of the qubit as a function of the energy bias of the qubit $\varepsilon(f_x) = 2\Phi_0 I_p f_x$. The sinusoidal current in the tank coil, indicated by the wavy line, drives the bias of the qubit. The starting point of the cooling (heating) cycles is denoted by blue (red) dots. The resonant excitation of the qubit due to the high-frequency driving, characterized by Ω_{R0}, is indicated by two green arrows and by the Lorentzian depicting the width of this resonance. The relaxation of the qubit is denoted by the black dashed arrows. The inset shows a schematic of the qubit coupled to an LC circuit. The high frequency driving is provided by an on-chip microwave antenna. **(b)** SEM picture of the superconducting flux qubit prepared by shadow evaporation technique.

states corresponding to persistent currents of amplitude I_p flowing clockwise and counterclockwise. When operated in the vicinity of the degeneracy point, $f_x \equiv \Phi_{\rm x}/\Phi_0 - 1/2 \approx 0$, where $\Phi_{\rm x}$ is the magnetic flux applied to the qubit loop and $\Phi_0 = h/2e$ the flux quantum, the Hamiltonian of the qubit in the basis of the persistent current states reads

$$H = -\frac{1}{2}\varepsilon(f_x)\sigma_z - \frac{1}{2}\Delta\sigma_x \ . \tag{1}$$

Here σ_x, σ_z are Pauli matrices, Δ is the tunneling amplitude, and $\varepsilon(f_x) = 2\Phi_0 I_p f_x$ is the energy bias. The energy levels of the isolated qubit, separated by $\Delta E(f_x) = \sqrt{\varepsilon^2(f_x) + \Delta^2}$ are shown in Fig. 1. The qubit is driven by a high-frequency field with frequency ω_d and coupled via a mutual inductance M to a low-frequency tank circuit with frequency $\omega_T \simeq 2\pi \times 20$ MHz $\ll \Delta/\hbar$. Both circuit to the qubit can be included at this stage via their contributions to the external flux Φ_x. Since the eigenfrequency of the tank circuit, ω_T, is much lower than the level spacing of the qubit, the oscillations of the current in the tank circuit can be treated in an adiabatic approximation, i.e., the current in the tank circuit shifts the bias flux of the qubit by $\Phi_x(t) = M[I_{dc} + I_{\rm rf}(t)]$.

The system mimics the Sisyphus mechanism of damping (cooling) and amplification (heating) known from quantum optics[12]. This mechanism is illustrated in Fig. 1. Here we describe the damping (cooling, hence marked in blue) for a situation where the driving is red-detuned, $\hbar\omega_d < \Delta E$; the amplification (marked in red) for blue-detuning can be described in an analogous way. The oscillations of the current in the tank circuit, $I_{\rm rf}(t)$, lead to oscillations of $\varepsilon(f_x)$ around a value determined by the *dc* component, I_{dc}. In the first part of the cycle, when the qubit is in the ground state, the current shifts the qubit towards the resonance, $\Delta E = \hbar\omega_d$, i.e., the energy of the qubit grows due to work done by the LC circuit. Once the system reaches the vicinity of the resonance point, the qubit can get excited, the energy being provided by the high-frequency driving field. With parameters adjusted such that this happens at the turning point of the oscillating trajectory, the qubit in the excited state is now shifted by the current away from the resonance, such that the qubits energy continues to grow. Again the work has to be provided by the LC circuit. The cycle is completed by a relaxation process which takes the qubit back to the ground state. The maximum effect is achieved when the driving frequency and relaxation rate are of the same order of magnitude. If the relaxation is too slow the state is merely shifted back and forth adiabatically during many periods of oscillations. Note that the complete cycle resembles the ideal Otto-engine thermodynamic cycle[14].

Two types of measurements have been performed on the system. In the first the LC tank circuit is additionally driven near-resonantly by a low- frequency rf current, and the response of the LC circuit is detected using lock-in techniques. In these measurements we identify the influence of the high-frequency driven qubit on the effective quality factor and eigenfrequency of the tank circuit. We associate a reduction of the effective quality factor with cooling and identify regions in parameter space where the effect is optimized.

In the second type of measurements the low-frequency rf-driving is switched off, while the emission of the LC tank circuit is monitored by a spectrum analyzer. This analysis probes the influence of the qubit on the effective quality factor, and, most importantly, allows us to determine the energy stored in the tank circuit, i.e., its effective temperature. Thus we are able to demonstrate cooling or heating of the LC oscillator.

We start with a qualitative analysis of the first type of measurement. The LC tank circuit is driven by a current source with amplitude I_T^d. Then the amplitude, V_T, of the voltage oscillations across the tank circuit, which is measured in the experiment, is

$$V_T = \omega_T L_T I_T = Q\,\omega_T L_T I_T^d \ , \tag{2}$$

where $I_T = \sqrt{2\langle I_{\rm rf}^2\rangle} = Q I_T^d$ is the actual amplitude of the rf current in the inductance, and Q is the effective quality factor of the tank circuit. It is given by the ratio, $Q = 2\pi W_T/A$, between the energy stored in the tank, $W_T = L_T I_T^2/2$, and energy loss per period A. The latter is composed of two contributions, $A = A_T + A_{\rm Sis}$. The intrinsic losses of the tank are given by $A_T = 2\pi W_T/Q_0$, where Q_0 is the intrinsic quality factor of the tank circuit. The average work done by the tank on the qubit in one period, $A_{\rm Sis}$, can be estimated as follows: We consider the optimal situation when the oscillator brings the qubit into the resonance at the turning point of its trajectory (Fig. 1). We assume further that the state of the qubit is instantaneously "thermalized", with equal probabilities to remain in the ground state or to get excited. In the latter case, after leaving the area of resonance the qubit can relax with rate Γ_R. The probability of qubit relaxing during the time $0 < t < T$ (here $T = 2\pi/\omega_T$) within an interval dt is given by $dP = \exp(-\Gamma_R t)\,\Gamma_R dt$. Thus we obtain the average value of the work (taking into account the probability $1/2$ of the initial state to be excited)

$$\begin{aligned} A_{\rm Sis} &= M I_p I_T \int dP\,[1 - \cos(\omega_T t)] \\ &= M I_p I_T f(\Gamma_R, \omega_T) \ , \end{aligned} \tag{3}$$

where

$$f(\Gamma_R, \omega_T) \equiv \left(1 - e^{-2\pi\Gamma_R/\omega_T}\right) \frac{\omega_T^2}{\omega_T^2 + \Gamma_R^2} \ . \tag{4}$$

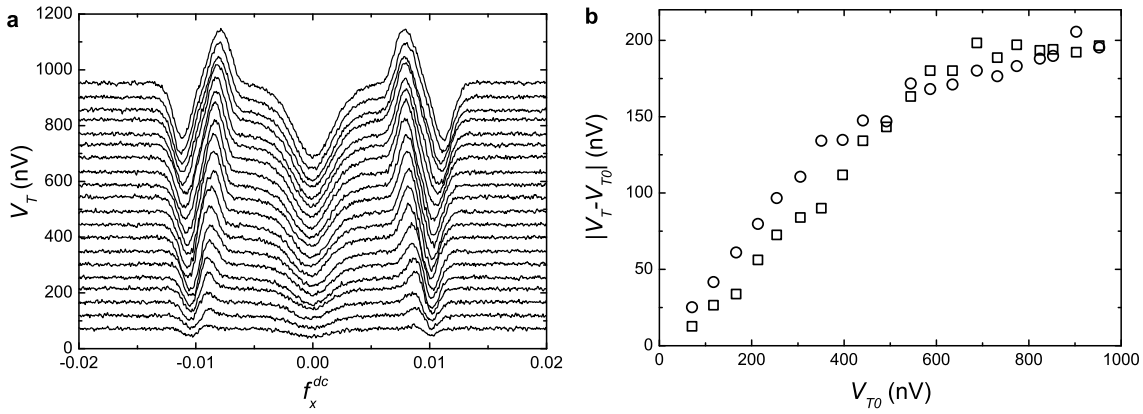

FIG. 2: **(a)** Amplitude of the rf tank voltage as a function of the dc magnetic bias of the qubit, f_x^{dc}, for a microwave driving frequency $\omega_d = 2\pi \times 14.125$ GHz and various amplitudes of the rf current driving the tank circuit. **(b)** The height of the peaks (solid squares) and dips (solid circles) as a function of the voltage amplitude of the unloaded tank circuit V_{T0}. The voltage V_{T0} is equal to, e.g., V_T taken at $f_x^{dc} = 0.02$ where the effect of the interaction between the tank circuit and the qubit is negligible. The height saturates near 200 nV.

This function demonstrates that the optimal situation for damping or amplification is reached when $\Gamma_R \sim \omega_T$. For the effective quality factor we obtain

$$Q = Q_0 \left(1 \pm \frac{A_{\rm Sis} Q_0}{2\pi W_T}\right)^{-1} = Q_0 \left(1 \pm \frac{M I_p Q_0 \omega_T f(\Gamma_R, \omega_T)}{\pi V_T}\right)^{-1} , \tag{5}$$

where $\pm$ stand for the damping/amplification. Substituting into Eq. (2) we arrive at

$$V_T - V_{T0} = \mp M \omega_T I_p Q_0 f(\Gamma_R, \omega_T)/\pi , \tag{6}$$

where $V_{T0} = Q_0 \omega_T L_T I_T^d$ is the voltage on the tank circuit far from the resonance. Eq. (6) provides the estimate for the increase/decrease of the tank voltage for large driving currents I_T^d, such that the qubit spends most of the time away from the resonant excitation area. For weaker driving, when the times spend away and within the excitation area are comparable, the damping effect becomes weaker.

Our results of the first type of experiment are shown in Fig. 2. The dips (peaks) correspond to the Sisyphus damping (amplification) of the tank circuit, i.e., to the decrease (increase) of the effective quality factor Q. The central dip is due to the shift of the oscillator frequency when the qubit is at it's degeneracy point[15] and is not related to the Sisyphus effect. We observe from Fig. 2b that the additional voltage saturates for large driving amplitudes at approximately 200 nV. Using this value and Eq. (6) we see that indeed the relaxation time is close to the period of oscillations, $1/\Gamma_R \approx 0.95T$.

The results for the second type of experiment are shown in Fig. 3. The comparison shows that at the bias point corresponding to maximum Sisyphus damping the resonant line widens in good agreement with the results for the driven LC circuit. At the bias point corresponding to maximum amplification the line narrows, showing a tendency towards lasing behavior. We can extract the quality factors in these two regimes, as well as for the bias point far from the resonance where no additional damping occurs. The comparison of the experimental results with Eq. (5) yields a quantitatively reasonable agreement.

Finally, the results displayed in Fig. 3 allow us to estimate the efficiency of the cooling or heating in the two regimes. Integrating the power spectra we observe that in the damping regime the number of photons in the LC circuit decreases by about 8% compared to the undamped case. The cooling effect was observed also for other microwave frequencies and lies in the range of $6\% - 13\%$. Thus there is only little cooling. One reason is that our system is optimized towards maximum Sisyphus damping rather than minimum cooling temperature. Indeed, damping is optimized when the resonant point is reached at the turning point of the oscillators trajectory. In this regime even a small reduction of the oscillators amplitude, i.e., a weak cooling, suffices to switch the whole mechanism off. We expect to be able to optimize in future experiments the system towards efficient cooling as well.

To develop the discussion further we model the Sisyphus damping as an additional effective bath coupled to the oscillator, which we characterize by a quality factor $Q_{\rm Sis}$ and temperature $T_{\rm Sis}$. The standard analysis gives the total quality factor and temperature, $Q^{-1} = Q_0^{-1} + Q_{\rm Sis}^{-1}$ and $TQ^{-1} = T_0 Q_0^{-1} + T_{\rm Sis} Q_{\rm Sis}^{-1}$, respectively. Here T_0 is the

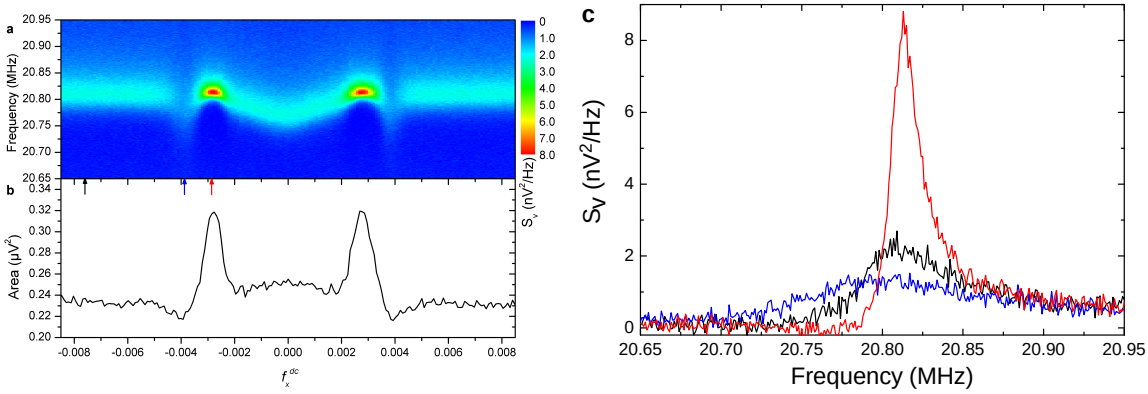

FIG. 3: **(a)** Spectral density of the voltage noise in the LC circuit, $S_V(\omega)$, measured when the low-frequency rf-driving is switched off while the high-frequency qubit driving is fixed at $\omega_d = 2\pi \times 6$ GHz. S_V is shown as a function of frequency (vertical axis) and normalized magnetic flux in the qubit $f_x^{\rm dc}$ (horizontal axis). **(b)** The integral, $\int S_V(\omega) d\omega$, evaluated using the data from panel **(a)** as a function of $f_x^{\rm dc}$. The integral is directly proportional to the number of quanta (effective temperature) of the tank circuit. At optimal dc bias $f_x^{\rm dc}$ the effective temperature T of the oscillator is lower than the temperature T_0 away from the resonance, $(T_0 - T)/T_0 = 0.08$, corresponding to an 8% cooling. **(c)** Spectral density $S_V(\omega)$ measured at three different values of $f_x^{\rm dc}$ corresponding to damping (blue), amplification (red), and away from the resonance (black). These values of $f_x^{\rm dc}$ are marked, respectively, by blue, red, and black arrows in panel **(a)**.

temperature of the oscillator without Sisyphus damping, which in our case is determined mostly by the amplifier. Our data show that $Q \sim Q_0/2$. Thus the coupling strength of the Sisyphus mechanism is comparable to that of the rest of the environment, i.e., $Q_{\rm Sis} \approx Q_0 \approx 340$. In the present experiment it looks as if $T_{\rm Sis}$ were comparable with T_0 and we have only little cooling.

In contrast, in the amplification mode of our experiment the line gets much sharper, which formally can be expressed by choosing $Q_{\rm Sis}$ negative, $Q_{\rm Sis} \approx -600$. This means that if no other bath was present the system would show the lasing instability. Consistently, the Sisyphus mechanism, acting as an active medium with population inversion, is described by a negative temperature $T_{\rm Sis}$. Its value is not known, but we can get a lower bound for the effective temperature from the inequality $T/Q > T_0/Q_0$. It predicts an increase in temperature and number of photons by a factor ~ 2. The experiment shows a 36% increase, which demonstrates the expected trend, even though some quantitative discrepancy remains.

We now outline the theoretical analysis of the problem. Quantizing the oscillations in the tank circuit we arrive at the Hamiltonian

$$\begin{aligned} H &= -\frac{1}{2}\,\varepsilon\left(f_x^{dc}\right)\sigma_z - \frac{1}{2}\,\Delta\sigma_x - \hbar\Omega_{R0}\cos(\omega_d t)\,\sigma_z \\ &\quad + \hbar\omega_T\, a^\dagger a \;+\; g\,\sigma_z\left(a + a^\dagger\right) \;. \end{aligned} \tag{7}$$

where the coupling constant is $g = MI_pI_{T,0}$, and $I_{T,0} = \sqrt{\hbar\omega_T/2L_T}$ is the amplitude of the vacuum fluctuation of the current in the LC oscillator. The third term of Eq. (7) describes the high-frequency driving with amplitude Ω_{R0}. After transformations to the eigenbasis of the qubit and some approximations appropriate for the considered situations (and described in the Appendix) the Hamiltonian reduces to

$$\begin{aligned} H &= -\frac{1}{2}\,\Delta E\,\sigma_z + \hbar\Omega_{R0}\cos\left(\omega_d t\right)\cos\zeta\,\sigma_x + \hbar\omega_T\, a^\dagger a \\ &\quad + \; g\sin\zeta\,\sigma_z\left(a + a^\dagger\right) - \frac{g^2}{\Delta E}\cos^2\zeta\,\sigma_z\left(a + a^\dagger\right)^2 \;, \end{aligned} \tag{8}$$

with $\Delta E \equiv \sqrt{\epsilon^2 + \Delta^2}$ and $\tan\zeta \equiv \varepsilon/\Delta$. Thus we obtain the effective Rabi frequency $\Omega_{R0}\cos\zeta$ and the effective constant of qubit-oscillator linear coupling $g\sin\zeta$. As we need both these terms for the Sisyphus cooling the qubit should be biased neither at the symmetry point nor very far from it. The second order term $\propto g^2$ is responsible, e.g., for the qubit-dependent shift of the oscillator frequency[15].

To account for the effects of dissipation we consider the Liouville equation for the density operator of the system including the two relevant damping terms,

$$\dot\rho = -\frac{i}{\hbar}\,[H, \rho] + L_Q\,\rho + L_R\,\rho \;. \tag{9}$$

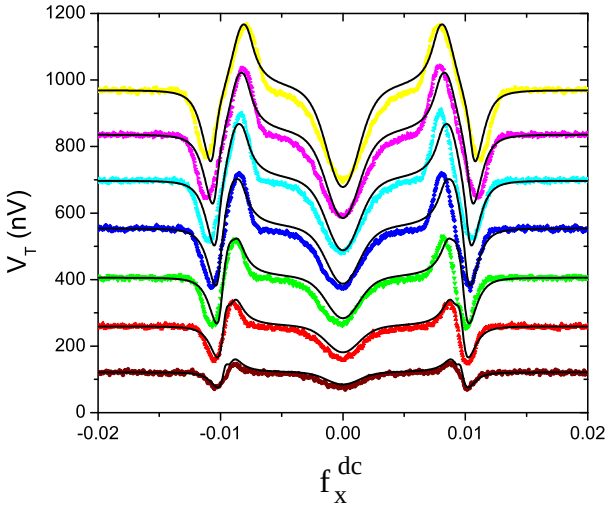

FIG. 4: Color lines: experimental data. Black lines: numerical solution of Eqs. (9) for $\Omega_{R0} = 2\pi \times 0.5$ GHz, $\Gamma_R = 1.0 \cdot 10^8 s^{-1}$, $\Gamma^*_\varphi = 5.0 \cdot 10^9 s^{-1}$. The central dip is due to the quadratic coupling term in (8) which causes a shift of the oscillator frequency[15].

As far as the qubit is concerned we consider spontaneous emission with rate Γ_R and pure dephasing with rate Γ^*_φ. Hence, we have

$$L_Q\,\rho \;=\; \frac{\Gamma_R}{2}\left(2\sigma_-\rho\sigma_+ - \rho\sigma_+\sigma_- - \sigma_+\sigma_-\rho\right) + \;\frac{\Gamma^*_\varphi}{2}\left(\sigma_z\rho\sigma_z - \rho\right)\;. \tag{10}$$

We neglect the excitation rate since the qubit's energy splitting exceeds the temperature. Thus the standard longitudinal relaxation time T_1 is given by $T_1^{-1} = \Gamma_R$. The rates Γ_R and Γ^*_φ may depend on the working point, i.e., on ζ, which in turn is determined by the driving frequency ω_d by the condition $\hbar\omega_d \approx \Delta E$. The rates should describe the dissipation around these values of ζ. It should be mentioned that pure dephasing is frequently caused by the $1/f$ noise[16], for which the Markovian description is not applicable. We hope, however, that the main features are still captured provided Γ^*_φ is chosen properly.

The resonator damping term can be written in usual form[17],

$$L_R\,\rho = \frac{\kappa}{2}\left(N_{\rm th}+1\right)\left(2a\rho a^\dagger - a^\dagger a\rho - \rho a^\dagger a\right) + \frac{\kappa}{2}N_{\rm th}\left(2a^\dagger\rho a - aa^\dagger\rho - \rho aa^\dagger\right), \tag{11}$$

where $\kappa = \omega_T/Q_0$ characterizes the strength of the resonator damping, and $N_{\rm th} = [\exp(\hbar\omega_T/k_BT) - 1]^{-1}$ is the thermal average number of photons in the resonator. We solve the master equation (9) numerically in the quasi-classical limit, i.e., for $n \equiv \langle a^\dagger a\rangle \gg 1$, and for various choices of the unknown parameters Γ_R, Γ^*_φ, and Ω_{R0}. As the system is harmonically driven, we determine the response of the observables/density matrix at the driving frequency, and, finally, find the amplitude of the driven voltage oscillations across the tank circuit. As shown in Fig. 4 by fitting the system parameters within a reasonable range we reproduce well the experimental findings. We should mention that a good fit can be obtained for a relatively wide range of values of the Rabi frequency Ω_{R0} and pure dephasing rate Γ^*_φ, provided we keep their product roughly constant. On the other hand, Γ_R is determined rather accurately.

The Sisyphus damping by a superconducting qubit analyzed in this paper can also be applied to nanomechanical systems[18,19,20,21]. With proper optimization towards minimum cooling temperature one could cool a mechanical resonator which would enable, e.g., ultra-sensitive detection applications like MRFM[22] with quantum limited precision.

---

[1] Nakamura, Y., Pashkin, Y. A. & Tsai, J. S. Coherent control of macroscopic quantum states in a single-cooper-pair box. *Nature* **398**, 786–788 (1999).

[2] Vion, D. *et al.* Manipulating the quantum state of an electrical circuit. *Science* **296**, 886–889 (2002).
[3] Chiorescu, I., Nakamura, Y., Harmans, C. & Mooij, J. Coherent quantum dynamics of a superconducting flux qubit. *Science* **299**, 1869–1871 (2003).
[4] Wallraff, A. *et al.* Strong coupling of a single photon to a superconducting qubit using circuit quantum electrodynamics. *Nature* **431**, 162–167 (2004).
[5] Chiorescu, I. *et al.* Coherent dynamics of a flux qubit coupled to a harmonic oscillator. *Nature* **431**, 159–162 (2004).
[6] Il'ichev, E. *et al.* Continuous monitoring of rabi oscillations in a josephson flux qubit. *Phys. Rev. Lett.* **91**, 097906 (2003).
[7] Blais, A., Huang, R., Wallraff, A., Girvin, S. M. & Schoelkopf, R. J. Cavity quantum electrodynamics for superconducting electrical circuits: An architecture for quantum computation. *Phys. Rev. A* **69**, 062320 (2004).
[8] Martin, I., Shnirman, A., Tian, L. & Zoller, P. Ground state cooling of mechanical resonators. *Phys. Rev. B* **69**, 125339 (2004).
[9] Rabl, P., Shnirman, A. & Zoller, P. Generation of squeezed states of nanomechanical resonators by reservoir engineering. *Phys. Rev. B* **70**, 205304 (2004).
[10] Niskanen, A. O., Nakamura, Y. & Pekola, J. P. Information entropic superconducting microcooler (2007). ArXiv:0704.0845v1.
[11] Hauss, J., Fedorov, A., Hutter, C., Shnirman, A. & Schön, G. Single-qubit lasing and cooling at the rabi frequency (2007). ArXiv:cond-mat/0701041v5.
[12] Wineland, D. J., Dalibard, J. & Cohen-Tannouji, C. Sisyphus cooling a bound atom. *J. Opt. Soc.* **B9**, 32–42 (1992).
[13] Mooij, J. E. *et al.* Josephson persistent-current qubit. *Science* **285**, 1036–1039 (1999).
[14] Quan, H. T., Liu, Y. X., Sun, C. P. & Nori, F. Method for direct observation of coherent quantum oscillations in a superconducting phase qubit. *Phys. Rev. E* **76**, 031105 (2007).
[15] Greenberg, Y. S. *et al.* Method for direct observation of coherent quantum oscillations in a superconducting phase qubit. *Phys. Rev. B* **66**, 224511 (2002).
[16] Ithier, G. *et al.* Decoherence in a superconducting quantum bit circuit. *Phys. Rev. B* **72**, 134519 (2005).
[17] Gardiner, C. W. & Zoller, P. *Quantum noise* (Springer, 2004), 3-d edn.
[18] Naik, A. *et al.* Cooling a nanomechanical resonator with quantum back-action. *Nature* **443**, 193–196 (2006).
[19] Blanter, Y. M., Usmani, O. & Nazarov, Y. V. Single-electron tunneling with strong mechanical feedback. *Phys. Rev. Lett.* **93**, 136802 (2004).
[20] Blencowe, M. P., Imbers, J. & Armour, A. D. Dynamics of a nanomechanical resonator coupled to a superconducting single-electron transistor. *New J. Phys.* **7**, 236 (2005).
[21] Bennett, S. D. & Clerk, A. A. Laser-like instabilities in quantum nano-electromechanical systems. *Phys. Rev. B* **74**, 201301 (2006).
[22] Sidles, J. A. *et al.* Magnetic resonance force microscopy. *Rev. Mod. Phys.* **67**, 249–265 (1995).

M.G. was supported by Grants VEGA 1/0096/08 and APVV-0432-07. We further acknowledge the financial support from the EU (RSFQubit and EuroSQIP).

Correspondence and requests for materials should be addressed to M.G. (email: grajcar@fmph.uniba.sk).

Appendix

After transformation to the eigenbasis of the qubit the Hamiltonian (7) becomes

$$\begin{aligned} H &= -\frac{1}{2}\,\Delta E\,\sigma_z - \hbar\Omega_{R0}\cos(\omega_d t)\,(\sin\zeta\,\sigma_z - \cos\zeta\,\sigma_x) \\ &+ \hbar\omega_T\,a^\dagger a + g\,(\sin\zeta\,\sigma_z - \cos\zeta\,\sigma_x)\left(a + a^\dagger\right) , \end{aligned}$$

with $\tan\zeta = \varepsilon/\Delta$ and $\Delta E \equiv \sqrt{\varepsilon^2 + \Delta^2}$. Because of the large difference of the energy scales between the qubit and the oscillator, $\Delta E \gg \hbar\omega_T$, we can drop within the usual rotating wave approximation (RWA) the longitudinal driving term $-\hbar\Omega_{R0}\cos(\omega_d t)\sin\zeta\,\sigma_z$. On the other hand, we retain the transverse coupling term, $-g\cos\zeta\,\sigma_x\left(a + a^\dagger\right)$, but transform it by employing a Schrieffer-Wolff transformation, $U_S = \exp(iS)$, with generator $S = (g/\Delta E)\cos\zeta\,\left(a + a^\dagger\right)\,\sigma_y$, into a second order longitudinal coupling. The Hamiltonian then reduces to the form (8).